R. Vijaykumar
K. J. Waldron
M. J. Tsai
Department of Mechanical Engineering
The Ohio State University
Columbus, Ohio 43210

Geometric Optimization of Serial Chain Manipulator Structures for Working Volume and Dexterity

Abstract

Broadly speaking, the regional structure of a manipulator, which consists of the three inboard joints and their associated members, determines the workspace shape and volume.

The orientation structure, which for a six-degrees-of-freedom manipulator consists of the three outboard joints and members, determines the geometric dexterity or orientation potential of the manipulator. It is possible to determine the optimal dimensions of the regional structure for a given total length, using straightforward geometric arguments. By the use of the spherical counterpart of Grashof's theorem formulated by Freudenstein (1964–65), it is also possible to show that there is an optimum geometry of the orientation structure.

Two methods of characterizing geometric dexterity are utilized in this paper. The first is the concept of a dexterous workspace, *which is a portion of the workspace within which the hand may assume any orientation. Although the dexterous workspace is a very useful concept for theoretical purposes, it is of limited practical utility because mechanical joint motion limits usually preclude its existence in real industrial robot structures. The second method of characterizing geometric dexterity is to trace the portion of the workspace within which the hand can assume a specified orientation.*

In this paper, the geometric conditions for the existence of a dexterous workspace are formulated for geometrically optimum, six-revolute manipulator structures. The optimization criteria used include freedom from geometric singularities. We show that for an optimal geometry, singular positions can be completely excluded with small reductions of the joint motion ranges. These reductions have a negligible effect on the geometric performance of the system.

1. Introduction

Recently, many optimization techniques that concentrate chiefly on workspace volume have been applied to manipulator workspaces. Roth (1975) was one of the first researchers to investigate the relationship between kinematic geometry and manipulator workspaces. Since then, there have been several attempts to delineate and analyze workspaces: Shimano and Roth (1976); Kumar and Waldron (1981, 1980); Sugimoto and Duffy (1981*a*, 1981*b*, "to appear"); Gupta and Roth (1982); and Tsai and Soni (1981). Yang and Lee (1982, 1983, 1984) and Lee and Yang (1983) have established performance criteria for manipulators on which optimization techniques have been based. It is felt that the same conclusions can be reached more easily by studying the geometry of the manipulator structure (Vijaykumar 1985). It is extremely difficult to develop a theory that exhausts all possibilities, but the basis for such a procedure is established in this paper. This study is restricted to six-degrees-of-freedom serial chain manipulators, although the basic principles can easily be applied to any robot geometry.

The manipulator structure can be subdivided into a regional structure and an orientation structure. The *regional structure,* or transport structure, transports the hand to the required position. This involves the first

The authors wish to acknowledge the support of the National Science Foundation, Mechanical Systems Program, grant number MEA 8304735.

The International Journal of Robotics Research,
Vol. 5, No. 2, Summer 1986

Fig. 1. Geometric modeling —parameters of member i.

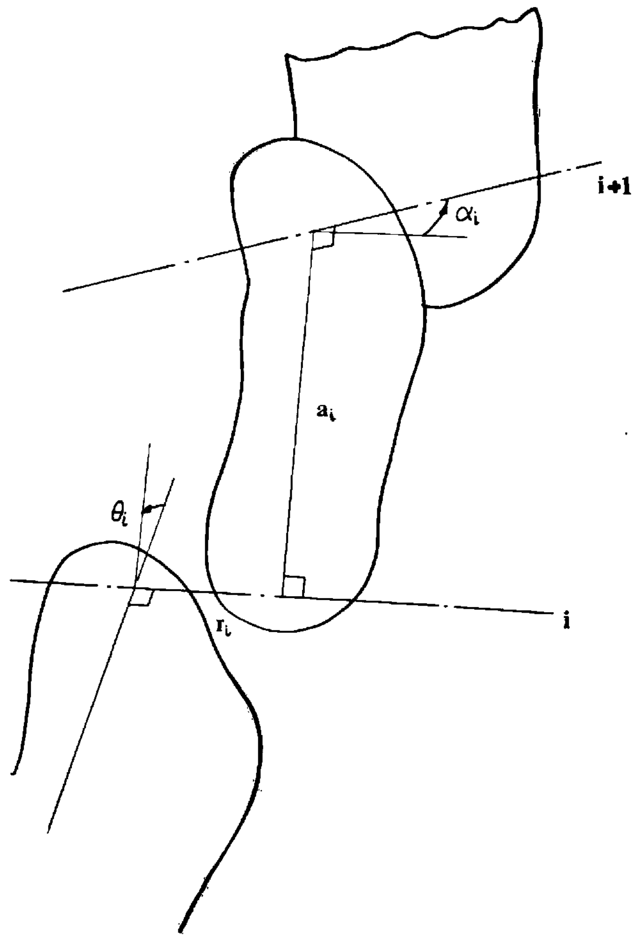

three links and joints in a six-degrees-of-freedom manipulator. These joints are called the *inboard joints*. The *orientation structure* consists of the *outboard joints* and performs the function of orienting the hand as desired.

The regional structure (Tsai and Soni 1981) consists of the arm and the elbow; the wrist joints comprise the orientation structure. Ideally, the inboard joints can move the reference point to the desired position, and the outboard joints permit the hand to assume the desired orientation by rotating the hand about an axis through the reference point. In other words, the translational and rotational components of motion are decoupled. This is not generally the case, however. Fortunately, it is possible to make this coupling weak, and most practical robot manipulator geometries illustrate this fact.

The operating region or workspace of a manipulator is characterized by a reachable workspace and a dexterous workspace (Kumar and Waldron 1981). The *reachable workspace* is defined as the volume or space within which a reference point on the hand (end effector) can be made to coincide with any point in space. The *dexterous workspace* is the volume within which the robot hand has complete manipulative capability. With a reference point in the dexterous workspace, the hand can be completely rotated about any axis through that point. Geometric dexterity is an important index of performance for a manipulator. For a general purpose manipulator, the objective is to maximize the volume of the reachable workspace and at the same time have the dexterous workspace as large a fraction of the reachable workspace as possible. It should be noted, however, that real manipulators with joint motion limits rarely have dexterous workspaces. Nevertheless, the concept is useful for design optimization.

In this discussion, it is assumed that all joint axes are either successively parallel or perpendicular to each other: i.e., all twist angles (α_i) are either 0 degrees or 90 degrees. In addition, for each member either the joint offset (r_i) *or* the link length (a_i) is zero. (This notation is shown in Fig. 1.) It is assumed that there are no limits on joint rotation, although this restriction will not be adhered to later in the discussion to arrive at more general conclusions. The orientation structure first deals with the objective of maximizing the dexterity of the wrist. In Section 3, the transport structure is optimized with the intention of maximizing the reachable workspace.

2. The Orientation Structure

The range of orientations achieved by the hand is at a maximum when the axes of the last three joints intersect at right angles: $\alpha_4 = \alpha_5 = 90$ degrees. In this configuration, if there are no joint motion limits, the hand can be rotated completely about any line through R, the point of concurrence of the three axes. This can be proved by considering the spherical indicatrix of axes 4, 5, and 6 with an arbitrarily oriented hypothetical axis i through point R. This axis is fixed in space

Fig. 2. The spatial 4-R linkage with axes 4, 5, 6, and i.

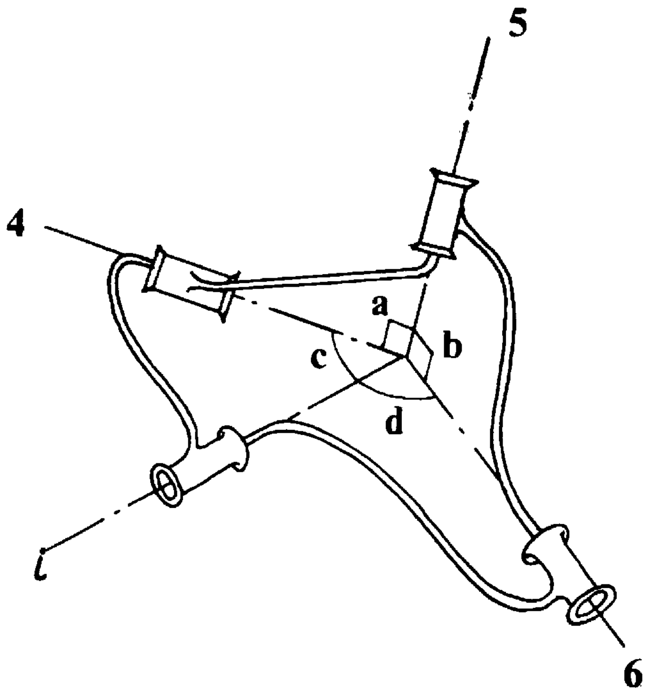

Fig. 3. Spherical indicatrix formed by axes 4, 5, 6, and i.

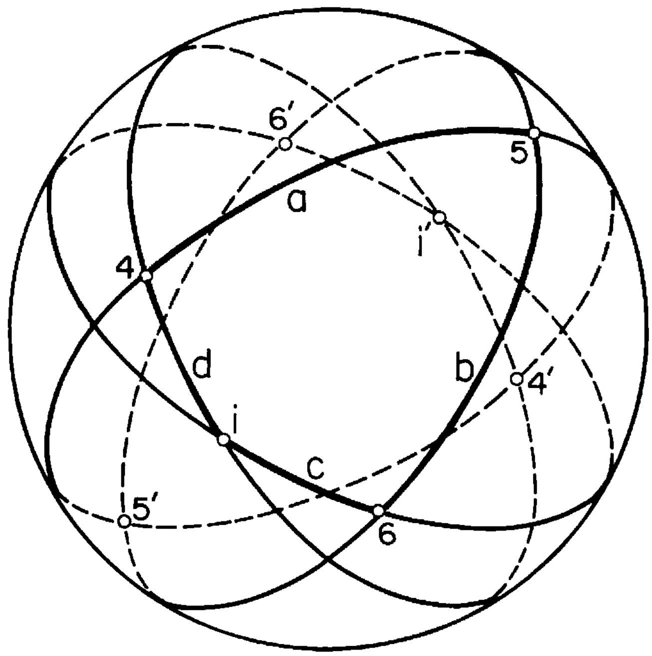

with respect to the world coordinates (see Fig. 2). If point R is stationary, links 1, 2, and 3 are stationary, and the only nonzero joint rates are those corresponding to axes 4, 5, and 6. The spherical Grashof criterion (Freudenstein 1964–65) is analogous to the planar Grashof criterion except that the link lengths between adjacent joints in the planar four-bar linkage are replaced by the angles between adjacent joint axes in the spherical four-bar linkage.

In Fig. 3, $a = \alpha_4 = 90$ degrees, and $b = \alpha_5 = 90$ degrees. The angles of the links in a spherical mechanism can always be replaced by their supplements. Hence c and d are less than or equal to 90 degrees. Clearly, either c or d is the smallest link angle and the largest link angle is 90 degrees. Therefore, the sum of the largest and the smallest link angles is always less than the sum of the other two link angles, so the spherical Grashof criterion is satisfied. The two joints adjacent to the smallest link angle (c or d) can rotate completely. Since one of these two joints is always joint i, complete rotation about an arbitrarily oriented axis (through the point of concurrence) is possible. Conversely, if either of these angles (α_4 or α_5) is less than 90 degrees, there will always be rotation axis directions for which the smallest angle is not adjacent to the rotation axis—specifically the rotation axis direction that is normal to both axis 4 and axis 6. Thus, the above condition is both necessary and sufficient.

If the reference point P were located (defined) at the point of concurrence of axes 4, 5, and 6, each reachable point in space would be one at which the hand could rotate completely through 360 degrees about any axis through that point. In other words, every reachable point would belong to the dexterous workspace (Kumar and Waldron 1980). However, the point of interest on the hand (the reference point) is not usually at the point of concurrence. Hence P is not coincident with R. This means that rotation about an axis through P requires rotation about axes 1, 2, and 3. Thus the coupling between the regional and the orientation structures comes into play, and the rotation about an axis through P may now be limited. The dexterous workspace no longer coincides with the reachable workspace, but it is still optimal for the concurrence of joint axes 4, 5, and 6.

The presence of motion limits does not invalidate this argument. In a planar four-bar linkage, the joints

Fig. 4. A. Generating curve where the first two joint axes are orthogonal and do not intersect. B. Generating curve where the first two joint axes are orthogonal and intersect.

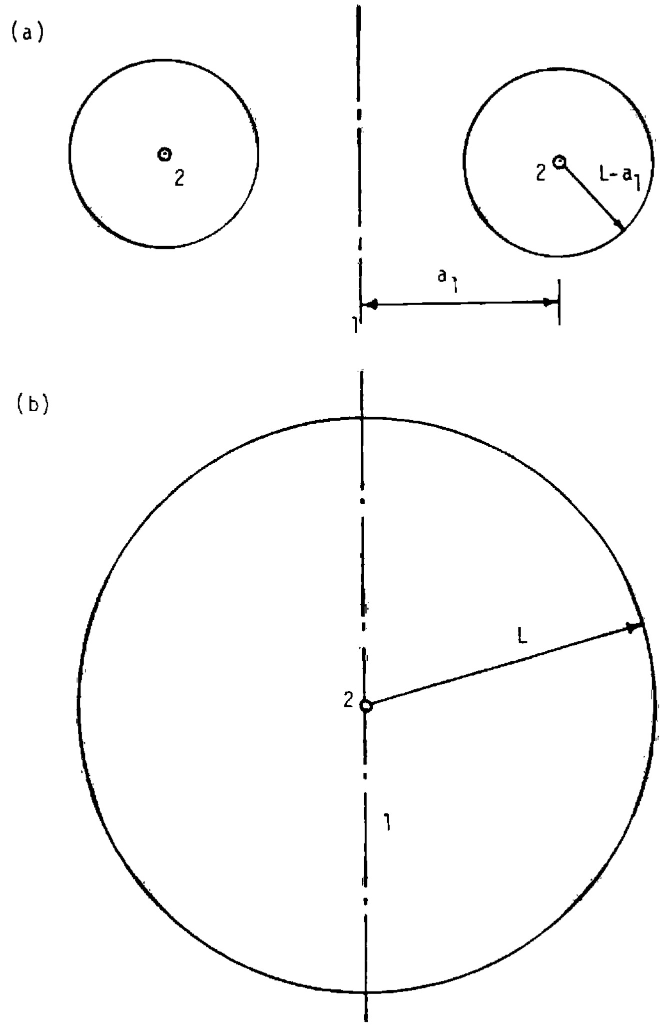

opposite to the ones that rotate completely can rock through an angle of 180 degrees or less. This is also true in the spherical case. If axes 4 and 6 can rotate through 360 degrees and axis 5 can execute the range $0 \leq \theta_5 \leq 180$ degrees, the range of orientations that can be assumed by the hand is not affected. Any further restrictions on the joint rotations will reduce the dexterity of the manipulator. Nevertheless, the optimum configuration for the outboard joints is one in which axes 4, 5, and 6 are concurrent and successively orthogonal. By application of the spherical sine and cosine rules, it is possible to show that for a given range of rotation about axis 4, say, the range of rotation about an arbitrary axis 4 through the concurrency point is maximized when axes 4 and 5 are orthogonal. Similar arguments apply to the other axes.

It should be noted that although some industrial robots have rotation capability about axis 5 approaching 180 degrees, it is usually in the range of -90 degrees $\leq \theta_5 \leq 90$ degrees, which does not satisfy the above requirement.

3. The Regional Structure

It is convenient to define the length of the manipulator as L, where

$$L = \sum_i (a_i + r_i)$$

and either a_i or $r_i = 0$. The inboard members will be optimized on the basis of workspace volume for the *same manipulator length.* Care is also taken to insure that there are no voids in the reachable workspace. In practice, however, the designer often feels the need for small voids to reduce interference with the structure. This problem varies with every manipulator and therefore is beyond the scope of this study.

It is easy to see that the workspace is symmetric about axis 1. Thus, the workspace can be described by considering its intersection with a radial plane through the axis of symmetry. In a cylindrical coordinate system, this plane is the $R - Z$ plane and $R = 0$ is the axis of symmetry. Lee and Yang (1983) describe this intersection as a circular projection on the $R - Z$ plane. In addition, if $\alpha_1 = 90$ degrees, the workspace is symmetric about another axis perpendicular to axis 1 passing through the intersection of the normal between axes 1 and 2 with axis 1.

Consider the situation where axes 1 and 2 are orthogonal: $\alpha_1 = 90$ degrees. For the first link, there are two possible cases: $a_1 \neq 0$ and $a_1 = 0$. Fig. 4 shows the curves generated by forcing the manipulator into extreme positions in each of these two cases. The workspace in the first case is a torus: the generating curve is a circle of radius $L - a_1$ and the center of the circle moves about axis 1 in a circle of radius a_1.

When $a_1 = 0$, the workspace is a sphere of radius L. If $a_1 \neq 0$, a family of tori is generated, but each torus

Fig. 5. Generating curves when first two axes are parallel.

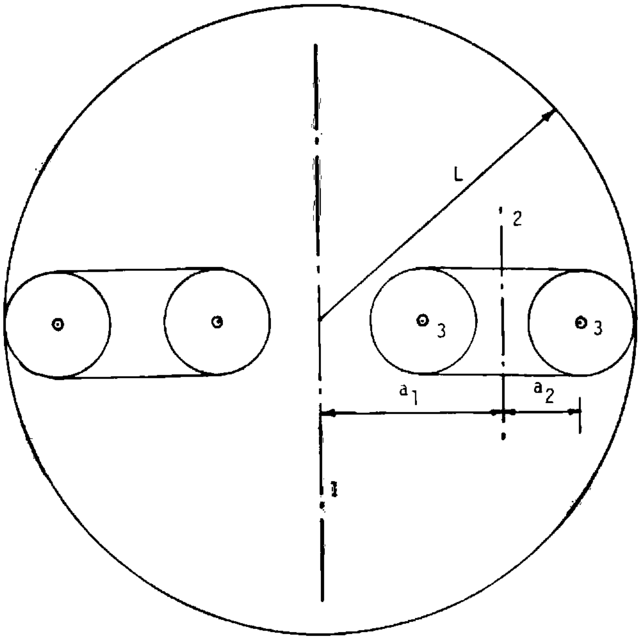

is within the volume of this sphere of radius L and the volume of the torus decreases as a_1 increases. Thus for a given L, the maximum workspace volume is obtained when $a_1 = 0$ and axes 1 and 2 intersect.

If $\alpha_1 = 0$ degrees, the first two axes are parallel. In this case, the third axis cannot be parallel to axes 1 and 2, because (see the optimum orientation structure of Section 2) the manipulator would always be reciprocal to a zero pitch screw axis through R parallel to axes 1, 2, and 3 (i.e., a geometrically singular structure) (Waldron, Wang, and Bolin, 1984). This is the reason that the numerous four- and five-degrees-of-freedom designs available commercially with parallel axes 1, 2, and 3 do not lend themselves to expansion to six degrees of freedom. On the other hand, if the third axis is perpendicular to the second, the right circular torus of Fig. 4 is distorted into a toroid (see Fig. 5). For a given L, the volume of this toroid is always less than that obtained when the first two axes intersect at right angles. This is true regardless of the value of a_1.

The preceding argument still remains valid, even if the restriction of no mechanical motion limits on the joints were removed, although the shape of the workspace would change. Thus the optimum workspace *volume* is obtained for a manipulator whose joints are all rotary joints and the first two joint axes intersect at right angles.

Fig. 6. A. Generating curve of a workspace whose first two joint axes are orthogonal with r_2 non-zero. B. Maximum attainable volume of the same.

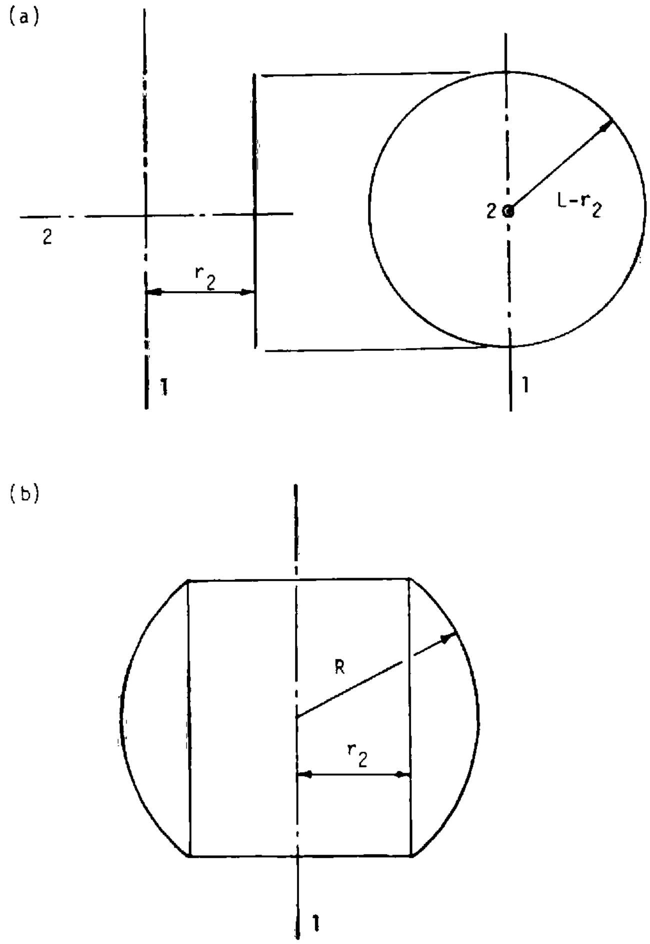

Consider now link $2 - r_2$, a_2, and axis 3. If r_2 were nonzero irrespective of whether a_2 is zero or not, the resulting generating curve would be a circle with a radius $L - r_2$. The maximum achievable workspace would be a sphere of radius R and volume V given by

$$R = \sqrt{(L - r_2)^2 + r_2^2};\; V = \frac{4\pi}{3}(L^2 - 2r_2L + 2r_2^2)^{3/2}.$$

The workspace has a cylindrical void of radius r_2 (see Fig. 6). Without this offset ($r_2 = 0$), the maximum volume is that of a sphere of radius L and is obviously larger.

Fig. 7. *Two optimal manipulator geometries.*

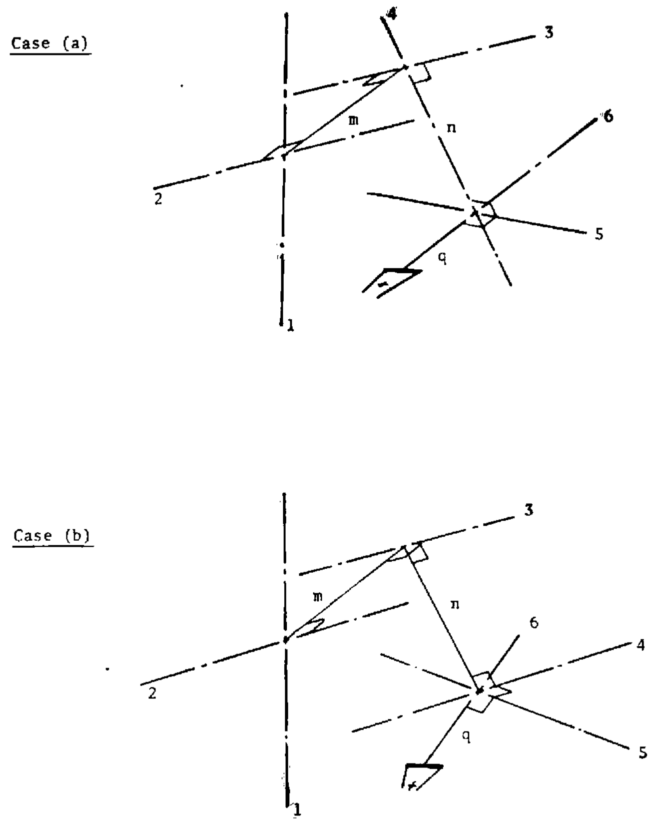

Thus, whether axes 2 and 3 are perpendicular or parallel, $r_2 = 0$ is required for an optimum configuration. If a_2 is zero, axis 3 intersects axis 2 at 90 degrees ($\alpha_2 = 0$ degrees, as this is a degenerate case in which axes 2 and 3 coincide). A problem of geometric singularity is caused by axis 3 intersecting with axis 2 at the point of intersection of axes 1 and 2 (axes 1, 2, and 3 are concurrent) (Waldron, Wang, and Bolin, 1984). If we consider the optimum configuration for the orientation structure (where axes 4, 5, and 6 are concurrent), the manipulator is always reciprocal to a zero pitch screw axis through the two points of concurrence. If $a_2 \neq 0$ and $\alpha_2 = 90$ degrees (axis 3 is at 90 degrees to axis 2), joint 3 is subjected to large twisting moments about an axis perpendicular to axis 3, as in most practical applications, the load on the manipulator hand is usually in the vertical direction (especially in any pick-and-place operation). Although this arrangement is geometrically viable, practically, $\alpha_2 =$ 0 degrees is a better choice, especially as the workspaces in both cases are identical.

This elimination process leaves the possibility of axis 3 being parallel to axis 2 with $r_2 = 0$ and $a_2 \neq 0$. Thus, the optimum arrangement for the regional structure is one in which axes 1 and 2 are perpendicular and intersecting and axis 3 is parallel to axis 2.

4. The Geometrically Optimum Structure

In Section 2, we noted that the optimal structure required axes 4, 5, and 6 to be concurrent. In Section 3, we concluded that axes 1 and 2 should be perpendicular and intersecting and axis 3 should be parallel to axis 2. The geometry of link 3 still remains undecided. Mechanical difficulties preclude the possibility of axis 4 intersecting axis 3 normally at a point that is far from the plane of the regional structure. This plane is normal to axes 2 and 3 and includes the intersection of axes 1 and 2. This arrangement results in large torsional moments at the elbow, although geometrically it is a viable one. Also, an argument based on an analysis similar to the one illustrated in Fig. 6 can be made against a nonzero r_3—the offset on axis 3 should be made zero for an optimal structure.

If the offset on axis 3, r_3, is zero, then there are three possibilities that can be considered (Fig. 7) for an optimal structure.

1. Axis 4 is parallel to axis 3 ($\alpha_3 = 0$ degrees).
2. Axis 4 is perpendicular to axis 3 and intersects it ($\alpha_3 = 90$ degrees and $a_3 = 0$).
3. Axis 4 is at right angles to axis 3 ($\alpha_3 = 90$ degrees) with $a_3 \neq 0$.

The third option is not very appealing because it creates undesirable torsional loading on joint 3. Thus, we must decide between the first two options. Later, when geometrical singularities are considered in greater detail in Section 7, it will be shown that Case (a) in Fig. 7 is a better structure than Case (b). These two optimal structures are shown in figure 7. We can conclude that $|m - n| = q$ is geometrically the best possible configuration. As Fig. 8 shows, $|m - n| > q$ results in a spherical void in the workspace, and

Fig. 8. Relation of workspace boundaries to lengths of manipulator dimensions.

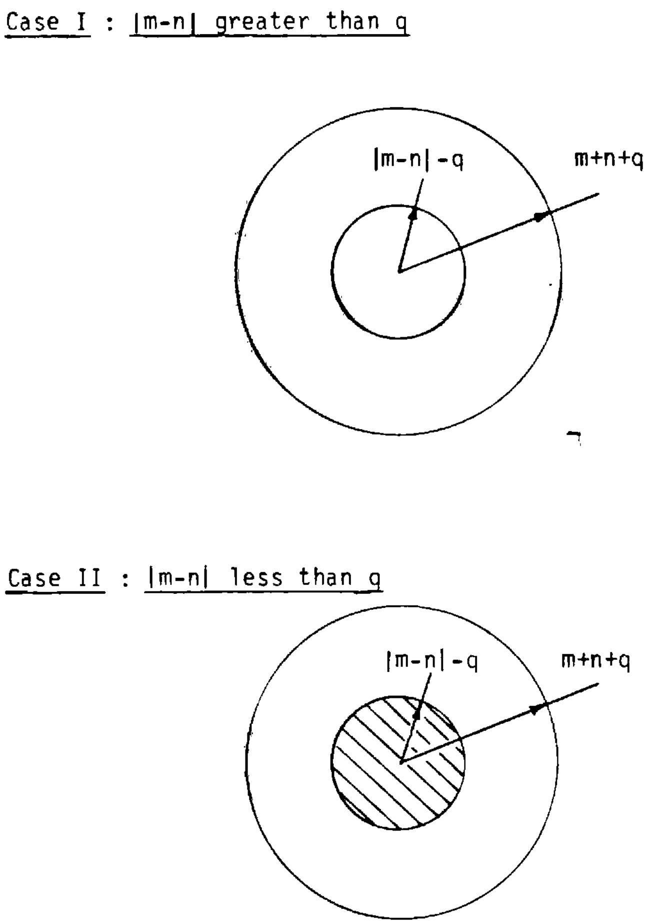

Fig. 9. The workspace for the optimal structure of Fig. 7.

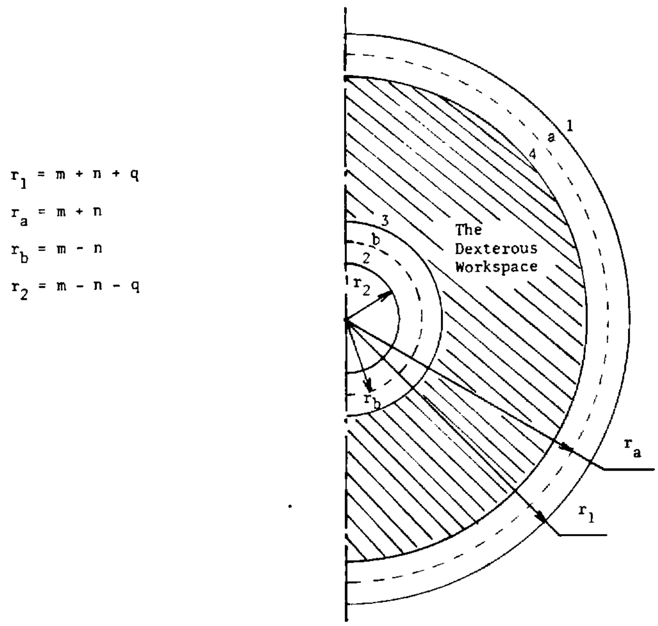

$|m - n| < q$ causes an overlap of workspace boundaries. Also the hand length q should be minimized. As we mentioned earlier, a zero value for q would be the best possible choice, but this is not usually mechanically feasible. The definition of the reference point could depend on the operation, and q cannot always be controlled. Thus, the ideal geometry is one in which $q = 0$ and $m = n$.

5. The Dexterous Workspace

Let us consider the two optimal structures shown in Fig. 7, which have a reachable workspace bounded by two concentric spheres of radii r_1 and r_2 (as shown in Fig. 9 for $m > n$). Figure 9 shows that the shaded workspace is a dexterous workspace. Then let us consider a hypothetical sphere S centered at any point Q in the reachable workspace with a radius q. If the reference point P is made to coincide with Q, the point of intersection of axes 4, 5, and 6 (point R) lies somewhere on this sphere (see Fig. 10). If, with P positioned at a point Q in space, R can be located at any arbitrary point on the hypothetical sphere S, Q belongs to the dexterous workspace. In such a case, axis 6 (along line PR) can lie along all generators of any cone with the vertex at P, and the hand can rotate completely about any of the infinity squared lines (axes) through Q (or P), as there is no limit on θ_6.

Now, if R is placed at any of the infinity squared points on S, suitable rotations about axes 4, 5, and 6 can force P to coincide with Q, the center of S. Based on the discussion in Section 2, we can easily see that the hand can assume any orientation and axis 6 can lie along any of the infinity of lines through R. A similar discussion can be found in Gupta and Roth (1982).

If R can be positioned at any arbitrary point on S (P can always be made to coincide with the center Q), Q belongs to the dexterous workspace. Furthermore, in an axisymmetric workspace, if R can be positioned on any point on the projection of the sphere S on the

Fig. 10. Dexterity of manipulators.

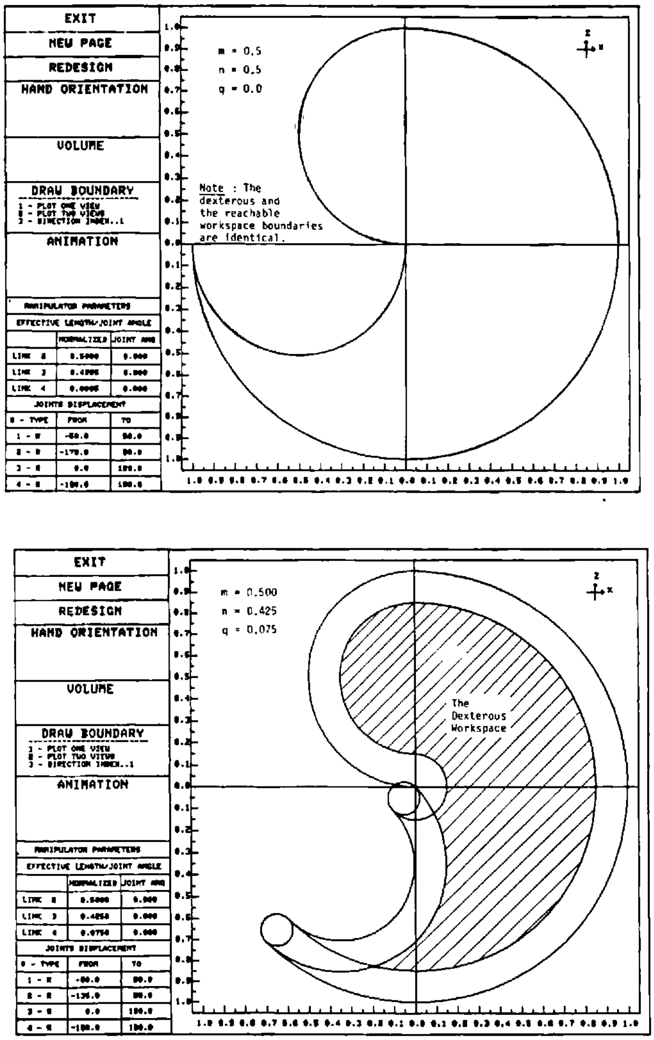

$R - Z$ plane (i.e. on or within the circle of radius q, centered at Q), R can be placed anywhere on the sphere. Hence, to prove that a point Q on the $R - Z$ plane belongs to the dexterous workspace, it is sufficient to prove that point R can be placed anywhere on or within the circle of radius q centered on Q.

In Fig. 9, point R can reach any point between the dotted lines a and b. Hence, all points belonging to the shaded region, which is defined by

$$r_b + q < r < r_a - q,$$

belong to the dexterous workspace. Also,

$$r_a = m + n$$

and

$$r_b = m - n.$$

Hence, the dexterous workspace is defined by

$$m - n + q < r < m + n - q.$$

If the reference point were located at the point of concurrence of axes 4, 5, and 6 (as discussed in Section 2), the dexterous and reachable workspaces would be identical, and

$$m - n < r < m + n$$

would determine the workspace.

6. Joint Limits

In this section, we explore the effect of mechanical joint limits on the reachable and dexterous workspaces of a manipulator. The manipulator structures, which have thus far been considered optimal, are used as an example (see Fig. 6).

First, limits are imposed on the inboard joints, and the effects of limits on θ_1, θ_2, and θ_3 are examined. Let joint 1 be limited by

$$-\theta_{1m} \leq \theta_1 \leq \theta_{1m},$$

where θ_{1m} is a positive value less than 180 degrees. The sweep of the arm is restricted, and the workspace is not axisymmetric anymore. θ_{1m} has no effect, however, on the cross-section of the workspace (the intersection of the workspace with an $R - Z$ plane). The volumes of the reachable and dexterous workspaces are proportional to θ_{1m}. Since the orientation and regional structures are not usually decoupled when θ_1 is close to θ_{1m} or $-\theta_{1m}$, the small rotation about axis 1, which is necessary to perform a 360 degree rotation of the hand about a general axis through the reference point, may not be possible. Of course, if $q = 0$, this effect is absent due to complete decoupling. In any case, it is

Fig. 11. A. Workspace for the optimal structure-effect of joint limits, with m = n, q = *0. B. Workspace for optimal structure with* |m − n| = q = *0.*

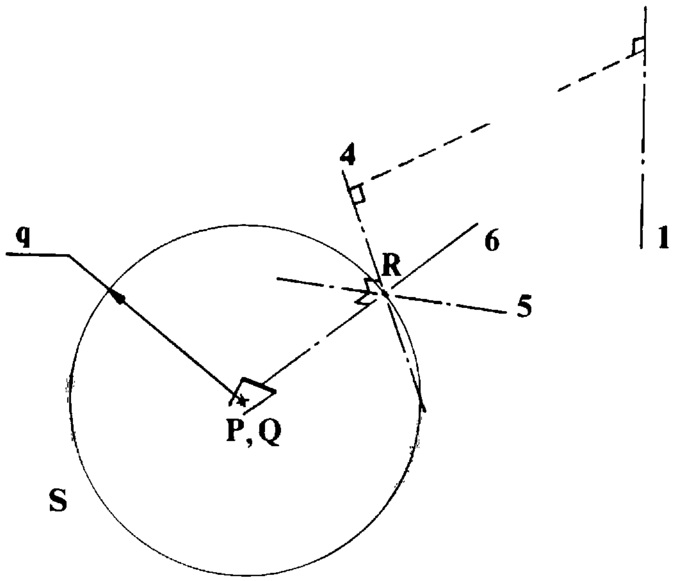

easy to see that the designer should strive to make $\theta_{1m} = 180$ degrees.

To simplify matters, let $q = 0$ and $m = n$. Now, consider the joint limits for axes 2 and 3 given by

$$-180^\circ \leq \theta_2 \leq 90^\circ$$

and

$$90^\circ \leq \theta_3 \leq 270^\circ \text{ for case (a)}$$

or

$$0^\circ \leq \theta_3 \leq 180^\circ \text{ for case (b).}$$

These ranges of joint rotation maximize the workspace volume and eliminate voids within the workspace. (It is possible to find many other combinations of joint limits that will satisfy this objective.) Fig. 11A shows the reachable workspace with these limits, with $q = 0$ and $m = n$. If $\theta_{1m} = 180$ degrees, this set of joint limits produces a spherical workspace of radius m that has no voids. Any reduction in the operating ranges of joint rotation will decrease the workspace volume and/or introduce voids in the workspace.

For a more general case, let $m \neq n$ and q be nonzero, but $|m - n| = q$. (This is the necessary condition to ensure the absence of voids and the overlapping of the workspace.) Here the joint limits for θ_2 can be further reduced from the -180 to 90 degrees range without producing any voids in the workspace. In figure 11B, the workspace has been obtained for this case, assuming that there are no limits on the outboard joints. It is very easy to identify the dexterous workspace. In line with Section 5, all points within the shaded area belong to the dexterous workspace. In figure 11A the boundaries of the dexterous and reachable workspaces are identical.

In Section 2, it was proved that if joints 4 and 6 are capable of 360 degrees of rotation and joint 5 can rotate through at least 180 degrees, the hand can rotate completely about any axis through the reference point ($q = 0$). Though $-180 \leq \theta_6 \leq 180$ degrees can be found in practical designs in the robot industry, it is not always mechanically feasible to achieve 360 degree rotation of joint 4.

If,

$$0^\circ \leq \theta_4 \leq 180^\circ$$

and

$$0^\circ \leq \theta_5 \leq 180^\circ,$$

then complete rotation about i is possible given a general axis i through R (see Fig. 2) such that the angle formed with axis 6 is less than the angle formed with axis 4. (Refer to the spherical indicatrix for the wrist, shown earlier in Fig. 2.) If the angle is greater than 90 degrees, it can be replaced by its supplement in accordance with principles of spherical trigonometry. This is easily seen by using analogies with the planar $4 - R$ and the spherical Grashof criterion (Freudenstein 1964–65). In general, however, it is difficult to draw any conclusions about dexterity if outboard joint rotation is limited.

7. Geometric Singularities

The optimization process resulting in the structures shown in Fig. 7 involved consideration of geometric singularities. Care was taken not to make the structure a singular one. Yet there may be configurations in

Fig. 12. Singular configurations: case (a).

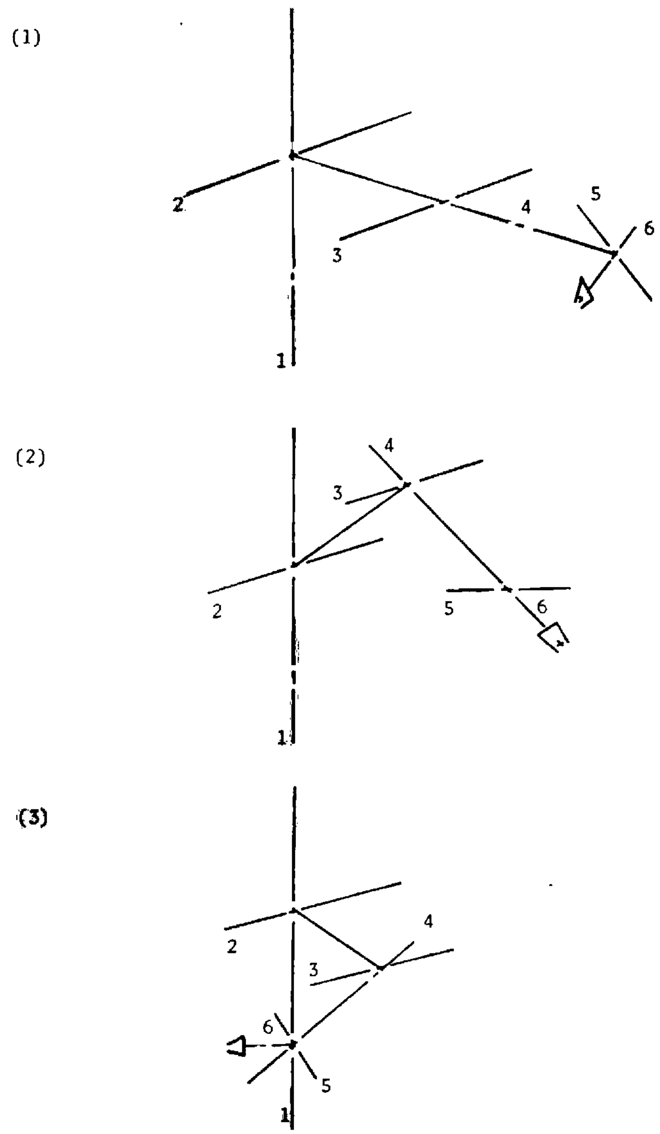

which the manipulator becomes singular, although, in general, the structure is not singular (Waldron, Wang, and Bolin 1984). This is a problem for control algorithms operating in world coordinates as the determinant of the Jacobian goes to zero. Some robots do have safety measures implemented in the software. However, it is possible to almost completely eliminate singular positions by limiting ranges of joint rotation, following the optimization of the structure.

The two examples from Fig. 7 have been considered here. The three conditions for singularity in Case (a) are (Waldron, Wang, and Bolin 1984):

1. $C\theta_3 = 0$.
2. $S\theta_5 = 0$.
3. $mC\theta_2 + nS(\theta_2 + \theta_3) = 0$.

Geometrically, these conditions can be interpreted very easily as follows (Fig. 12):

1. The elbow is either fully extended or doubled back, and axes 2, 3, and 4 are coplanar.
2. Axes 4 and 6 are coaxial.
3. The point of intersection of axes 4, 5, and 6 lies on axis 1.

Conditions 1 and 2 can be avoided by reducing joint ranges of axes 3 and 5 from

$$90° < \theta_3 \leq 270° \text{ to } (90° + \delta_3) < \theta_3 \leq 270° - \delta_3$$

and

$$0° < \theta_5 \leq 180° \text{ to } \delta_5 < \theta_5 \leq (180° - \delta_5),$$

when δ_3 and δ_5 are very small angles (see Section 6). This insures that conditions 1 and 2 are never satisfied. Condition 3 leads to a configuration where R, the point of concurrence of axes 4, 5, and 6, lies on axis 1. In practice, however, industrial robots can never achieve this configuration by reaching below axis 2 because the dimension (radius) of the base is substantial. However, it is possible for the point of concurrence of axes 4, 5, and 6 to lie on axis 1 above axis 2. This singular configuration cannot be eliminated by limiting joint rotations alone, and software traps are essential to prevent the manipulator from encountering this special configuration.

Similarly, in Case (b) the singularity equation can be broken down into three conditions:

1. $S\theta_3 = 0$.
2. $S\theta_5 = 0$.
3. $mC\theta_2 + nC(\theta_2 + \theta_3) = 0$.

These conditions can be interpreted geometrically in the same way as in Case (a) except that condition 1 requires axes 2, 3, and 4 to be parallel in addition to being coplanar.

Fig. 13. Singular configurations: case (b).

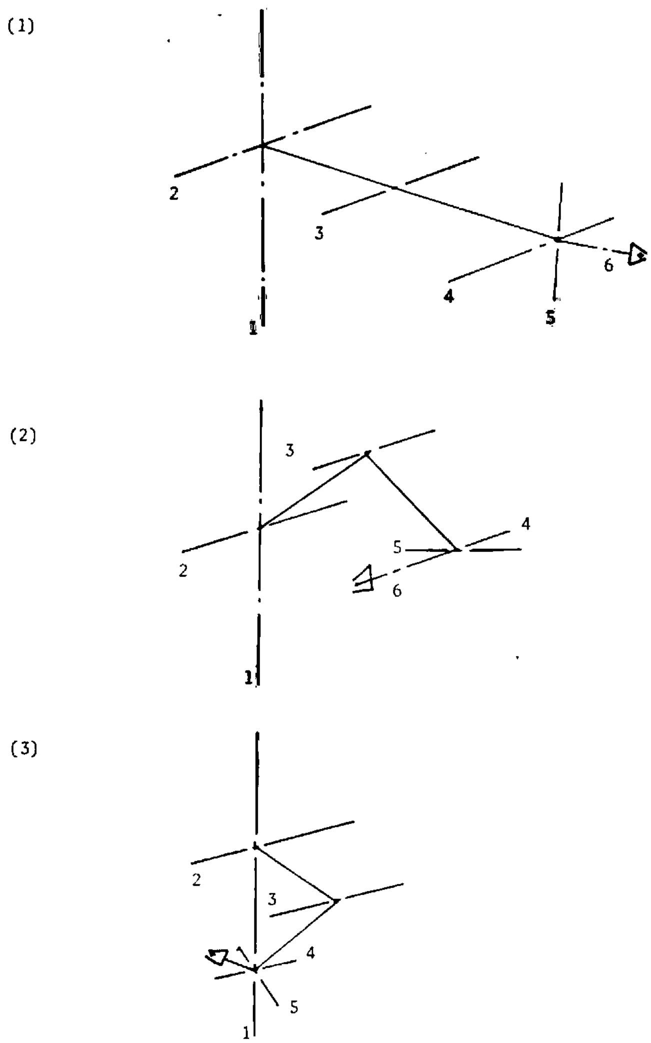

Imposing restrictions on joints 3 and 5,

$$\delta_3 < \theta_3 \leq 180^\circ - \delta_3$$

and

$$\delta_5 < \theta_5 \leq 180^\circ - \delta_5.$$

This precludes the possibility of the manipulator assuming a configuration satisfying conditions 1 or 2 (see Fig. 13). As in Case (a), condition 3 requires R to lie on axis 1, which can be encountered only if the manipulator reaches above axis 2 and the point of concurrence of axes 4, 5, and 6 lies on axis 1. Once more, the singular positions corresponding to condition 3 cannot be excluded.

Thus, it is possible to eliminate almost all singularities by modifying the ranges of joint rotation by a very small amount from the ranges specified in Section 6 without changing the workspace significantly.

An inspection of condition 2 in both cases reveals:

In Case (a), the manipulator cannot extend its wrist or bend it back along axis 4, as this would necessitate $\theta_5 = 0$ (or 180) degrees. This poses a very stringent restriction on the hand orientation during operation.

In Case (b), axis 4 and axis 6 cannot be permitted to assume a coaxial configuration, but this prevents the hand from assuming orientations that may be important (axis 6 cannot be directed perpendicular to the $R - Z$ plane).

Asada and Cro Granito (1985) suggested that alignment of the hand between these extremes may be optimal, depending on the application.

If the reference point is on axis 6 (i.e., $a_6 = 0$), Case (a) restricts the reach of the manipulator and prevents the wrist from assuming a radially outward orientation. For example, an operation involving tightening of bolts in an assembly line is one case where it is convenient to align axis 6 along the bolt axis and use the actuator on axis 6. Here, if the line of approach is along the radial direction (radial with respect to the $R - Z$ axis coordinates on the manipulator), Case (b) is naturally more attractive. Thus, it would seem that Case (b) is a better choice and it is not surprising that many industrial robots are built with this structure. Ultimately, of course, the choice depends on the type of operation and work station for which the robot is being designed.

8. Sliding Joints

Sliding joints are useless in the orientation structure as they do not allow rotation about any axis. Clearly, the use of sliding joints should be limited to the regional structure, where they can simplify the control algorithms with respect to the inversion of the Jacobian, and real time computations are reduced. Furthermore,

Fig. 14. A. Cylindrical workspace geometry obtained when joint 2 is a sliding coaxial with rotary joint 1. B. Spherical workspace geometry obtained when joint 3 is a sliding joint and joints 1 and 2 are orthogonally intersecting rotary joints. C. Rectangular workspace geometry obtained when joints 1, 2, and 3 are orthogonal sliding workspace joints.

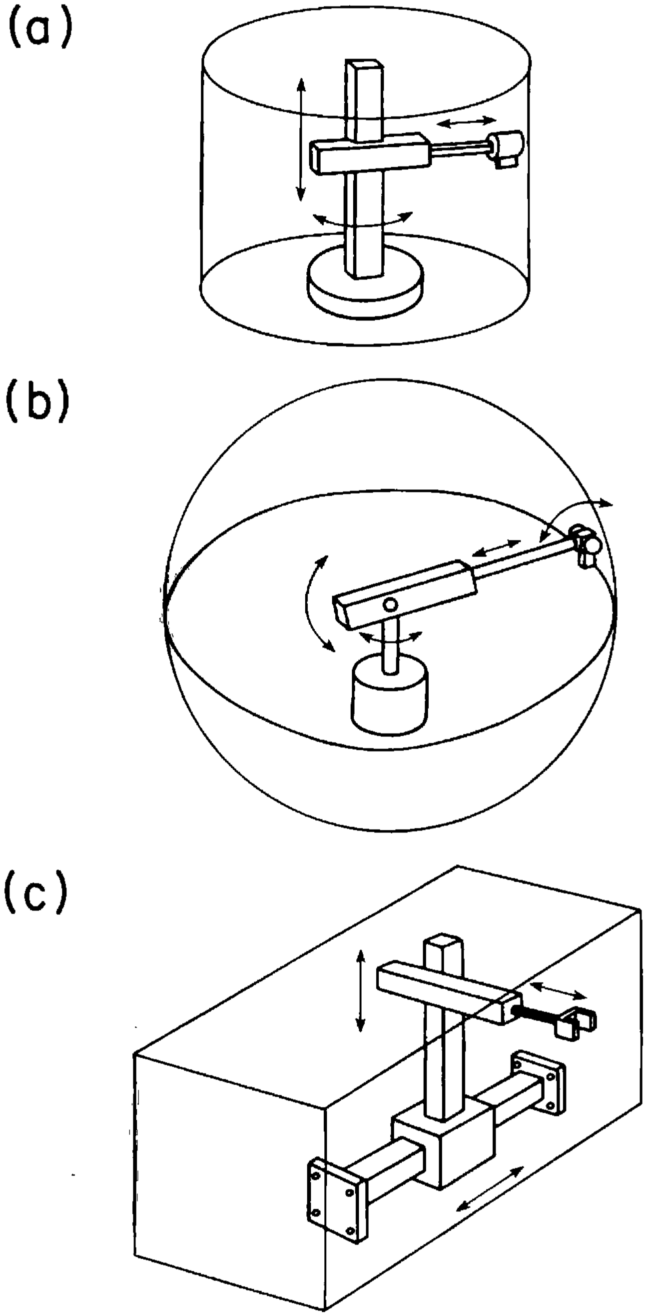

as the inboard joints do not participate in the orientation, we have some decoupling of the rotation and the translation equations. (As the outboard joints affect positioning in the general case, the decoupling is only partial.) However, use of rotating joints can achieve workspaces with smaller structural volumes as compared to those with sliding joints, and this is one of the principal reasons why revolute joints have been popular with robot manufacturers, despite relatively complex control requirements. Figure 14 shows some typical structures with prismatic joints and the associated workspaces.

9. Concluding Remarks

We have tried to demonstrate that geometric optimization of manipulator structures requires only simple arguments based on kinematic geometry or, in a few instances, statics. Although our discussion was limited almost entirely to serial structures with rotary joints, the same general principles apply to optimization of structures with other types of joints or with parallel chain configurations.

Although optimization of the regional structure has been presented before, a rigorous derivation of the optimal orientation structure and of the relationship of the dexterous workspace to hand length has not been previously attempted.

We have also tried to show that, for these simple geometries, geometrically singular positions can be largely excluded with minimal performance cost by the appropriate choice of joint motion limits.

References

Asada, H., and Cro Granito, J. A. 1985 (Mar. 25–28, St. Louis). Kinematic and static characterization of wrist joints and their optimal design. *Proc. 1985 IEEE Int. Conf. on Robotics and Automation*, pp. 244–250.

Freudenstein, F. 1964–65. Note on the type determination of spherical four bar linkages. *Invited Contribution of the 60th Birthday Anniversary on the Theory of Mechanisms for I. I. Artobolevski.*

Gupta, K. C., and Roth, B. 1982. Design considerations for manipulator workspace. *ASME J. Mechanical Design* 104(4):704–712.

Hunt, K. H. 1978. *Kinematic geometry of mechanisms.* Oxford: Clarendon Press.

Kumar, A., and Waldron, K. J. 1980. The dexterous work-

space. *Design Engineering Tech. Conf.* ASME paper No. 80-DET-108.
Kumar, A., and Waldron, K. J. 1981. The workspaces of a mechanical manipulator. *ASME J. Mechanical Design* 103(3):665–672.
Lee, T. W., and Yang, D. C. H. 1983. On the evaluation of manipulator workspace. *ASME J. Mechanisms, Transmissions and Automation in Design* 105(1):70–77.
Roth, B. 1975. Performance evaluation of manipulators from a kinematic viewpoint. *NBS Special Publication*:39–61.
Shimano, B. E., and Roth, B. 1976 (Warsaw, Poland). Ranges of motion of manipulators. *Proc. CISM-IFToMM Symp. Theory Pract. Robots Manipulators,* pp. 18–27.
Sugimoto, K., and Duffy, J. 1981*a*. Determination of extreme distances of a robot hand part 1: a general theory. *ASME J. Mechanical Design* 103(3):631–636.
Sugimoto, K., and Duffy, J. 1981*b*. Determination of extreme distances of a robot hand part 2: robot arms special geometry. *ASME J. Mechanical Design* 103(4):776–783.
Sugimoto, K., and Duffy, J. Special configuration of spatial mechanisms and robot arms. To appear in *Mechanism and Mach. Theory.*
Tsai, Y. C., and Soni, A. H. 1981. Accessible region and synthesis of robot arms. *ASME J. Mechanical Design* 103(4):803–811.
Vijaykumar, R., 1985. Robot manipulators—workspace and geometric dexterity. Master's Thesis, The Ohio State University, Columbus, Ohio.
Waldron, K. J., Wang, S. L., and Bolin, S. J. 1984. A study of the Jacobian matrix of serial manipulators. *Design Engineering Tech. Conf.* ASME paper no. 84-DET-109.
Yang, D. C. H., and Lee, T. W. 1982. Optimization of manipulator workspace, ed. W. J. Bock. *Robotic research and application.* ASME Book no. H00236.
Yang, D. C. H., and Lee, T. W. 1983. On the workspace of mechanical manipulators. *ASME J. Mechanisms, Transmissions and Automation in Design* 105(1):62–70.
Yang, D. C. H., and Lee, T. W. 1984 (July/August). Heuristic optimization in the design of manipulator workspace. *IEEE Trans. on Systems, Man and Cyber.* SMC 14(4).